Anisotropy of the energy gap in the insulating phase of the U-t-t' Hubbard model

Philipp Brune, Arno P. Kampf

Angaben zur Veröffentlichung / Publication details:

Brune, Philipp, and Arno P. Kampf. 2000. "Anisotropy of the energy gap in the insulating phase of the U-t-t' Hubbard model." *European Physical Journal B* 18 (2): 241–45. https://doi.org/10.1007/s100510070054.

Anisotropy of the energy gap in the insulating phase of the U-t-t′ Hubbard model

Ph. Brune[a] and A.P. Kampf

Institut für Physik, Theoretische Physik III, Elektronische Korrelationen und Magnetismus, Universität Augsburg, 86135 Augsburg, Germany

Abstract. We apply a diagrammatic expansion method around the atomic limit ($U \gg t$) for the U-t-t' Hubbard model at half filling and finite temperature by means of a continued fraction representation of the one-particle Green's function. From the analysis of the spectral function $A(\mathbf{k},\omega)$ we find an energy dispersion relation with a $(\cos k_x - \cos k_y)^2$ modulation of the energy gap in the insulating phase. This anisotropy is compared with experimental ARPES results on insulating cuprates.

PACS. 71.10.Fd Lattice fermion models (Hubbard model, etc.) – 71.27.+a Strongly correlated electron systems; heavy fermions – 71.30.+h Metal-insulator transitions and other electronic transitions

During the last decade of research work on high temperature superconductors angular resolved photoemission spectroscopy (ARPES) has played an important role in elucidating their electronic properties [1]. An understanding of the single particle properties in the normal state is a prerequisite for a theory of a mechanism for superconductivity as well as for transport properties. Over the years ARPES data have continuously provided surprises and new insights and thereby served as a guidance to theoretical developments. The observation of the $d_{x^2-y^2}$-shape of the energy gap, pseudogap structures in the metallic phase [2,3], strong anisotropies in the quasiparticle (qp) peak lineshapes and a possible partial destruction of the Fermi surface [4], or the unusual frequency and temperature dependence of the qp peakwidth [5] are examples for intriguing information obtained from ARPES experiments.

For the normal state an important goal is the description for the evolution with doping from the antiferromagnetic (AF) and insulating parent compounds to the overdoped superconductors. This demands control over the spectral features of the Mott-Hubbard insulating state as a starting point. Yet, it proved to be difficult to reproduce ARPES data for the single hole dispersion in the insulating cuprate $Sr_2CuO_2Cl_2$ [6] within t-J or Hubbard models. In particular, for momenta along the Brillouin zone (BZ) axis next-nearest neighbor (nnn) or even longer range hopping amplitudes had to be introduced to achieve a reasonable comparison to the measured spectra [7–15]. Even more striking are recent results on AF $Ca_2CuO_2Cl_2$ that demonstrated an anisotropy of the insulating energy gap which was claimed to follow closely a $d_{x^2-y^2}$-wave modulation along a remnant Fermi surface with a modulation amplitude of $\sim$ 300 meV comparable in magnitude to the AF exchange interaction [16,17]. It has been pointed out that a $d_{x^2-y^2}$ gap modulation might follow naturally in the context of a projected SO(5) theory [18] unifying antiferromagnetism and d-wave superconductivity by a symmetry principle [19].

In this paper we show that a $\gamma_d^2(\mathbf{k}) = (\cos k_x - \cos k_y)^2$ modulation of the AF energy gap is realized in the half-filled Hubbard model on a square lattice with nearest (nn) and nnn hopping amplitudes. This result is obtained in an analytic strong coupling expansion around the atomic limit following a recently proposed strategy with a mapping to a Jacobi continued fraction representation for the propagator [20]. Given that the Mott-Hubbard insulator is the appropriate starting point for studying the hole doping evolution in cuprates this intrinsic anisotropy may bear an important preformed structure for the doped metallic phase.

The single particle Matsubara Green's function for the Hubbard model is represented in terms of Grassmann fields γ^* and γ in the Feynman path integral representation by

$$G_{ij}(\tau\sigma|\tau'\sigma') = -\langle T_\tau c_{i\sigma}(\tau)\, c^\dagger_{j\sigma'}(\tau')\rangle = -\frac{1}{Z}\int [\mathrm{d}\gamma^*\,\mathrm{d}\gamma]\,\gamma_{i\sigma\tau}\,\gamma^*_{j\sigma'\tau'}\,\exp(-S[\gamma^*,\gamma]) \quad (1)$$

[a] e-mail: philipp.brune@physik.uni-augsburg.de

with the partition function Z and the action $S = S_{\rm kin} + S_{\rm atom}$ where

$$S_{\rm kin}[\gamma^*,\gamma] = -\int_0^\beta {\rm d}\tau \sum_{i,j,\sigma} t_{ij}(\gamma^*_{i\sigma\tau}\gamma_{j\sigma\tau} + {\rm h.c.}) \;, \quad (2)$$

$$S_{\rm atom}[\gamma^*,\gamma] = \int_0^\beta {\rm d}\tau \sum_{i,\sigma} \gamma^*_{i\sigma\tau}(\frac{\partial}{\partial\tau} - \mu)\,\gamma_{i\sigma\tau} + U\sum_i \gamma^*_{i\uparrow\tau}\gamma^*_{i\downarrow\tau}\gamma_{i\downarrow\tau}\gamma_{i\uparrow\tau} \quad . \quad (3)$$

Here, $c^\dagger_{i\sigma}$ creates an electron at site i with spin σ, and we restrict the hopping amplitudes t_{ij} to nn (t) and nnn (t') sites. U is the on-site Coulomb repulsion, μ the chemical potential, and $\beta = 1/T$ the inverse temperature.

The Green's function is evaluated diagrammatically in terms of a cumulant expansion around the atomic limit, *i.e.* an expansion in powers of t/U [21]. For clarity we outline the necessary calculational steps to derive this expansion in the path integral language in the same way as described by Pairault *et al.* [20]. One starts from the generating functional

$$G_{ij}(\tau\sigma|\tau'\sigma') = -\frac{\delta^2}{\delta J^*_a \delta J_b} \;\; \frac{1}{Z}\int [{\rm d}\gamma^*\,{\rm d}\gamma]\,\exp(-S[\gamma^*,\gamma]) \times \exp\;\; -\sum_{a'} J^*_{a'}\gamma_{a'} + \gamma^*_{a'}J_{a'} \;\Big]_{J=J^*=0} \;, \quad (4)$$

where $a = (i,\sigma,\tau)$, $b = (j,\sigma',\tau')$, etc. denote tripels of site, spin, and imaginary time indices. As early on suggested by Sarker [22] it is convenient to introduce auxiliary Grassmann fields $\{\psi^*_{i\sigma\tau}, \psi_{i\sigma\tau}\}$ by performing a Hubbard-Stratonovich transformation

$$G_{ij}(\tau\sigma|\tau'\sigma') = -\frac{\delta^2}{\delta J^*_a \delta J_b} \;\; \frac{1}{Z}\int [{\rm d}\psi^*\,{\rm d}\psi]\int [{\rm d}\gamma^*\,{\rm d}\gamma] \times \exp\;\; -\sum_{a',b'} t^{-1}_{a'b'}\psi^*_{a'}\psi_{b'} - S_{\rm atom}[\gamma^*,\gamma] \times \exp\;\; \sum_{a'}(\psi^*_{a'} - J^*_{a'})\gamma_{a'} + \gamma^*_{a'}(\psi_{a'} - J_{a'}) \;\Big]_{J=J^*=0} \quad (5)$$

with respect to the kinetic energy term equation (2). With a shift of the integration variables $\psi_a - J_a \rightarrow \psi_a$ one obtains

$$G_{ij}(\tau\sigma|\tau'\sigma') = -\frac{\delta^2}{\delta J^*_a \delta J_b} \;\; \frac{1}{Z}\int [{\rm d}\psi^*\,{\rm d}\psi]\int [{\rm d}\gamma^*\,{\rm d}\gamma] \times \exp\;\; -\sum_{a',b'} t^{-1}_{a'b'}(\psi^*_{a'} + J^*_{a'})(\psi_{b'} + J_{b'}) \times \exp\;\; \sum_{a'} \psi^*_{a'}\gamma_{a'} + \gamma^*_{a'}\psi_{a'} \times \exp\;\; -S_{\rm atom}[\gamma^*,\gamma] \Big|_{J=J^*=0} \;. \quad (6)$$

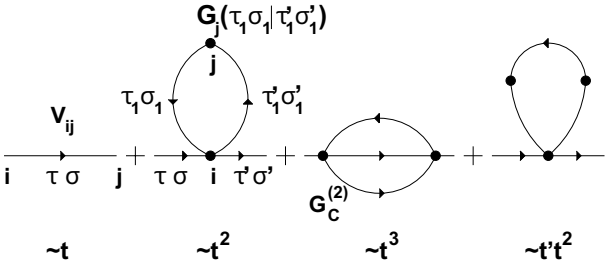

Fig. 1. Irreducible diagrams contributing to $G(\mathbf{k}, {\rm i}\omega_n)$ of the U-t-t' Hubbard model up to the order $(t/U)^3$. The vertices ($\bullet$) represent local n-particle cumulants $G^{(n)}_{\rm C}$. Each of the lines represents a hopping process with amplitude either t or t'.

The path integral over the fields $\{\gamma^*_{i\sigma\tau}, \gamma_{i\sigma\tau}\}$ is then written as

$$\frac{1}{Z_{\rm atom}}\int [{\rm d}\gamma^*\,{\rm d}\gamma] \exp\;\; \sum_{a'} \psi^*_{a'}\gamma_{a'} + \gamma^*_{a'}\psi_{a'} \times \exp\;\; -S_{\rm atom}[\gamma^*,\gamma] \;\; = \exp\;\; -\sum_n S^n_{\rm int}[\psi^*,\psi] \quad , \quad (7)$$

where $Z_{\rm atom}$ is the partition function with respect to the action $S_{\rm atom}$. The interaction part of the action is given by

$$S^n_{\rm int}[\psi^*,\psi] = -\frac{1}{(n!)^2}\sum_{\{a_n,b_n\}} \psi^*_{a_1}\ldots\psi^*_{a_n}\psi_{b_n}\ldots\psi_{b_1} \times G^{(n)}_{{\rm C}\,a_1\ldots a_n|b_n\ldots b_1} \;, \quad (8)$$

where the $G^{(n)}_{\rm C}$ denote local n-particle cumulants (connected Green's functions). From equation (6) one obtains the expression $G_{ij}(\tau\sigma|\tau'\sigma') = (\Gamma^{-1} - V)^{-1}_{ij}(\tau\sigma|\tau'\sigma')$ [20], where Γ denotes the self energy and $V_{ij}(\tau\sigma|\tau'\sigma') = -t_{ij}\,\delta_{\sigma\sigma'}\,\delta(\tau - \tau')$ is the non-interacting Green's function for the auxiliary fields, *i.e.* $\mathcal{V} = V + V\Gamma\mathcal{V}$. The Green's function of the auxiliary field is defined by

$$\mathcal{V}_{ij}(\tau\sigma|\tau'\sigma') = -\langle T_\tau \psi_{i\sigma\tau}\psi^*_{j\sigma'\tau'}\rangle = -\frac{1}{Z}\int [{\rm d}\psi^*\,{\rm d}\psi]\,\psi_a\psi^*_b \times \exp\;\; -\sum_{a',b'} t^{-1}_{a'b'}\,\psi^*_{a'}\psi_{b'} \times \exp\;\; -\sum_n S^n_{\rm int}[\psi^*,\psi] \quad . \quad (9)$$

From the expansion of the auxiliary Green's function in powers of t/U one obtains the diagrams contributing to $\Gamma_{ij}(\tau\sigma|\tau'\sigma')$ and thus also the diagrammatic expansion of the propagator $G_{ij}(\tau\sigma|\tau'\sigma')$ which is illustrated in Figure 1.

As is known from previous work on strong-coupling expansions for the Hubbard model [21,23] the Green's function calculated this way does not have the correct analytic properties, because higher order cumulants contain also higher order poles. This problem was circumvented in reference [20] by mapping the Green's function as calculated

by the diagrammatic expansion to a Green's function G_J in a finite Jacobi continued fraction representation [24]

$$G_J(z) = \cfrac{a_0}{z + b_1 - \cfrac{a_1}{z + b_2 - \cfrac{a_2}{z + \cdots - \cfrac{a_{N-1}}{z + b_N}}}} \qquad (10)$$

such that G_J has the same series expansion as G to the same order in t/U. We use this technique and apply it to the U-t-t' Hubbard model.

Specifically, we have calculated the Fourier transformed Green's function $G(\mathbf{k}, \mathrm{i}\omega_n)$ at half filling $\mu = \frac{U}{2}$ up to order $(t/U)^4$. While our independently obtained results agree with reference [20] for nn hopping only, in the case of a finite nnn hopping t' an additional tt'^2/U^3 diagram contributes to $G(\mathbf{k}, \mathrm{i}\omega_n)$ as shown in Figure 1. In this type of diagrams the vertices represent local n-particle cumulants $G_{\mathrm{C}}^{(n)}$ (connected Green's functions). Each line between two vertices represents a hopping process between two sites. In the absence of a Wick theorem for the local Green's functions the higher order cumulants must be calculated separately. The resulting algebraic expressions become very involved for higher order cumulants; for the performance of this diagrammatic expansion we have therefore developed a special purpose computer algebra code.

As a result we obtain a Jacobi continued fraction expression for G_J that has eight fraction levels, *i.e.* the coefficients a_N in equation (10) vanish for $N > 8$. This termination for G_J translates into eight simple poles. Each of the continued fraction coefficients a_i, b_i $(i = 1, \ldots, 8)$ is given by a fourth order polynomial in t/U or t'/U, respectively, with coefficients that depend on T, μ, U, and $\mathbf{k}$. The explicit result for G_J is accessible electronically [25]. In Figure 2 we show the corresponding spectral function

$$A(\mathbf{k}, \omega) = -\frac{1}{\pi} \operatorname{Im} G(\mathbf{k}, \omega + \mathrm{i}0^+) \qquad (11)$$

for different $\mathbf{k} = (k_x, k_y)$ along the path $(0,0) \to (\pi,\pi) \to (\pi,0) \to (0,0)$ in the first BZ. On the scale of this plot only six out of eight poles of $G_J(\mathbf{k}, \omega)$ carry significant and visible spectral weight.

In analyzing the spectrum we map out the dispersion of the lowest energy hole excitation, *i.e.* the dispersion of the first peak below the gap (marked by an arrow in Fig. 2). Its spectral weight is largest at the BZ center and drops monotonically towards (π, π). Figure 3 shows the peak dispersion for different temperatures. Upon cooling the system approaches the AF ordered ground state with a doubled unit cell and a reduced magnetic BZ (determined by $\cos k_x + \cos k_y \geq 0$). The dispersion along the zone diagonal approaches a perfectly symmetric shape with respect to the point $\mathbf{k}_d = (\frac{\pi}{2}, \frac{\pi}{2})$ on the magnetic BZ boundary reflecting the growing AF spin correlations. Remarkably, along the BZ axis the dispersion remains very flat at all temperatures. In fact, the dispersion along the axis is obtained flatter than in previous numerical studies of Hubbard or t-J models [7,12,26,27]. In units of the exchange coupling $J = 4t^2/U$ the total bandwidth of the energy dispersion is 1.58 for $T = 0.2t$, which is roughly consistent with experiment and previous calculations.

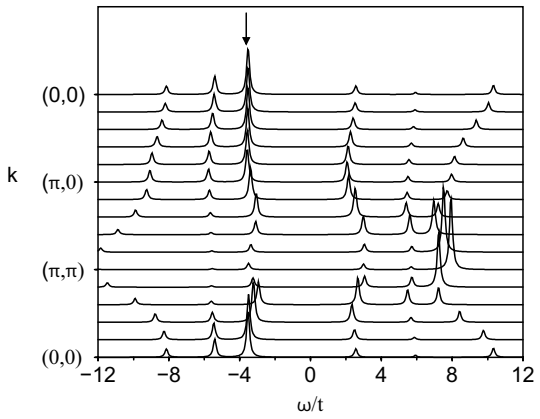

Fig. 2. Spectral function $A\mathbf{k}, \omega)$ of the half-filled U-t-t' Hubbard model as a function of ω along the path $\mathbf{k} = (0,0) \to (\pi,\pi) \to (\pi,0) \to (0,0)$ through the first Brillouin zone for $U = 10t$, $T = 0.2t$ and $t' = -0.45t$ as obtained from the strong coupling expansion to order $(t/U)^4$.

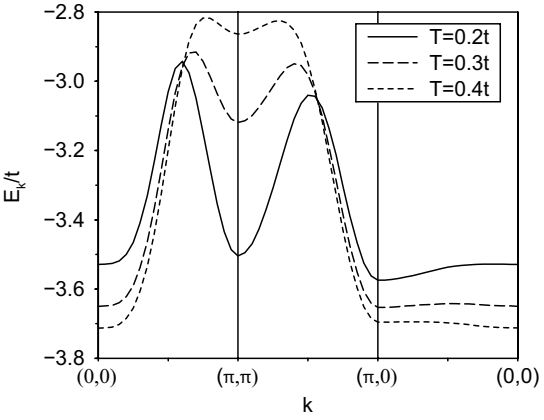

Fig. 3. Temperature dependence of the dispersion $E(\mathbf{k})$ of the low energy peak (marked by an arrow in Fig. 2) along a selected path in the first Brillouin zone for $U = 10t$ and $t' = -0.45t$.

In Figure 4 we compare our result for the single hole dispersion with the ARPES data on $Sr_2CuO_2Cl_2$ from reference [6]. For $U = 10t$ the parameters t and t' were chosen to obtain a best fit to the data. The overall agreement, in particular along the BZ axis, is quite satisfactory.

Hopping amplitudes beyond nnn hopping are found unnecessary for reproducing the flat dispersion along the BZ axis. ARPES experiments on insulating $Sr_2CuO_2Cl_2$ subsequent to reference [6] report different results on the flatness of the dispersion along this line [14,28]. This issue still seems experimentally unresolved (for a discussion see *e.g.* Ref. [29]), but it is interesting to note that the flat dispersion – in contradiction to previous theoretical

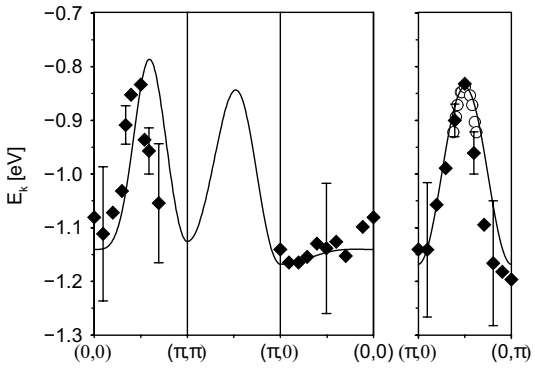

Fig. 4. A comparison with the ARPES dispersion for $Sr_2CuO_2Cl_2$ taken from reference [6] (black diamonds) and reference [17] (white circles). Error bars are shown at some selected experimental data points. The parameters in the theory were chosen as $U = 10t$, $T = 0.2t$, $t' = -0.45t$, and $t = 0.605$ eV.

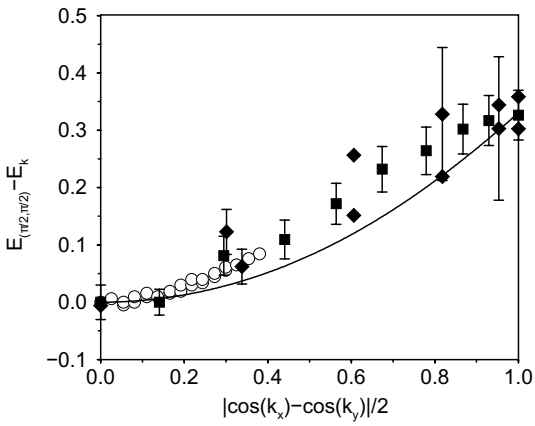

Fig. 5. Same data as in Figure 4 along the BZ path from $\mathbf{k}_d = (\pi/2, \pi/2)$ to $(\pi, 0)$, but here $E(\mathbf{k}_d) - E(\mathbf{k})$ is plotted as a function of $|\gamma_d(\mathbf{k})|/2$. In addition, ARPES data on $Ca_2CuO_2Cl_2$ (from Ref. [16]) are shown (black squares).

results – is obtained naturally within the presented strong-coupling theory for the Hubbard model with nnn hopping only.

The deviation of the theoretical result from the experimental data points along the BZ diagonal, *i.e.* the lack of symmetry with respect to $\mathbf{k}_d$ – as realized in the AF state – is due to the finite temperature. In fact, the range of applicability of the t/U expansion has a lower bound in temperature. (Following the arguments of Ref. [20] we estimate that our results are valid for $T > 0.16t$.) When the magnetic correlation length is much larger than the hopping range as given by the order of the t/U expansion, an accurate description of the single particle Green's function is no longer expected. The data were taken 100 K above the Néel temperature $T_N = 256$ K of $Sr_2CuO_2Cl_2$; at this temperature the magnetic correlation length is already as large as 250 Å as measured by neutron scattering [30]. Nevertheless, the flatness of the dispersion along the BZ axis in the t/U expansion is a robust and temperature insensitive feature.

In Figure 5 the calculated energy dispersion $E(\mathbf{k}_d) - E(\mathbf{k})$ of the lowest energy peak and the experimental data are plotted along the BZ path from $\mathbf{k}_d$ to $(\pi, 0)$ which is parameterized in the form $|\gamma_d(\mathbf{k})|/2$. Originally, the data of reference [16] (black squares) were anticipated to imply a $d_{x^2-y^2}$-modulation of the energy gap which in the parametrization of Figure 5 would translate into a straight line. The perfectly linear relation between $E(\mathbf{k}_d) - E(\mathbf{k})$ and $|\gamma_d(\mathbf{k})|$ along the chosen path would furthermore imply an unreasonable cusp-like feature of the dispersion on the magnetic BZ boundary. Indeed, the more recent data by Ronning *et al.* [17] (white circles in Fig. 5) resolve this problem and rather provide evidence for a quadratic dependence of the energy gap on $|\gamma_d(\mathbf{k})|$ in the vicinity of $\mathbf{k}_d$. Given the experimental error bars of reference [6] included in Figure 5 and in the absence of an error estimate for the recent data by Ronning *et al.* [17] our results are

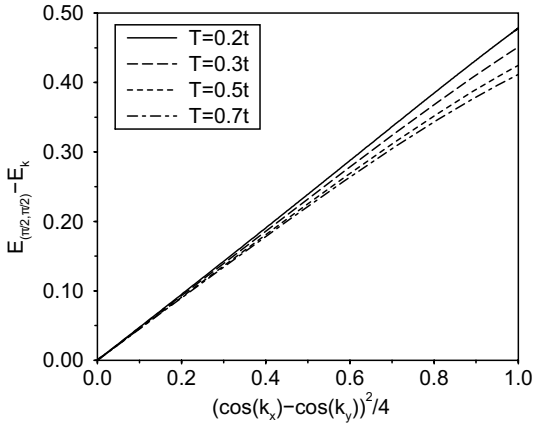

Fig. 6. Dispersion along the path from $\mathbf{k}_d = (\pi/2, \pi/2)$ to $(\pi, 0)$ relative to its value at $\mathbf{k}_d$ as a function of $(\cos k_x - \cos k_y)^2/4$ for different temperatures with $U = 10t$ and $t' = -0.4t$.

clearly compatible with experiment. With the same parameter set used for the fit of the ARPES dispersion in Figure 4 the gap modulation amplitude ~ 300 meV as measured in $Ca_2CuO_2Cl_2$ [16] is reproduced as well.

Figure 6 shows the temperature dependence of the gap modulation. In fact, when plotted *versus* $\gamma_d^2(\mathbf{k})$ it becomes evident that the gap approaches a perfect $\gamma_d^2(\mathbf{k})$ momentum dependence at low temperatures. For $t' = 0$ the modulation vanishes in the expansion up to the order $(t/U)^4$ because the $\mathbf{k}$ dependence of all diagrams to this order arises in the form $\cos k_x + \cos k_y$ for $t' = 0$ which vanishes on the BZ boundary for $t' = 0$. If diagrams of order $(t/U)^6$ or higher were taken into account, a small modulation is expected to appear also for $t' = 0$.

It is an interesting observation that the SDW mean-field solution of the U-t-t' Hubbard model, where the energy dispersion takes the form of two energy bands

$E_{\pm}(\mathbf{k}) = -4t' \cos k_x \cos k_y \pm \sqrt{\ ^2(\mathbf{k}) + \Delta^2}$, shows the same momentum dependence along the magnetic BZ boundary, since both are $\sim (\cos k_x)^2$ for $k_x = \pi - k_y$. Even though the SDW mean-field result does not agree with the experimentally obtained dispersion over the entire BZ [7], this observation clearly shows that it already captures some features of the strong-coupling result.

In summary, we have found in a strong coupling expansion to order $(t/U)^4$ that the energy gap in the insulating phase of the half-filled U-t-t' Hubbard model develops a $(\cos k_x - \cos k_y)^2$ modulation at low temperatures. Without the need to include hopping amplitudes beyond nnn an excellent fit is achieved for the single hole dispersion in $Sr_2CuO_2Cl_2$. With the same dispersion fit parameters also the calculated gap modulation amplitude compares well with the ARPES data. It is natural to expect that these spectral features in the insulator carry over to the metallic, doped case; the consequences and the connection to anisotropic pseudogap structures or even d-wave superconductivity remain yet to be understood.

We thank D. Duffy and F. Ronning for discussions and S. Pairault for sharing his insight into the efficient calculation of high order diagrams. This work was supported by the Deutsche Forschungsgemeinschaft through SFB 484.

References

1. For a review see Z.-X. Shen, D. Dessau, Phys. Rep. **253**, 1 (1995).
2. D.S. Marshall *et al.*, Phys. Rev. Lett. **76**, 4841 (1996); A.G. Loeser *et al.*, Science **273**, 325 (1996).
3. H. Ding *et al.*, Nature **382**, 51 (1996).
4. M.R. Norman *et al.*, Nature **392**, 157 (1998).
5. T. Valla *et al.*, Science **285**, 2110 (1999).
6. B.O. Wells *et al.*, Phys. Rev. Lett. **74**, 964 (1995).
7. D. Duffy, A. Moreo, Phys. Rev. B **52**, 15607 (1995).
8. A. Nazarenko *et al.*, **51**, 8676 (1995).
9. B. Kyung, R. Ferrell, Phys. Rev. B **54**, 10125 (1996).
10. V.I. Belinicher *et al.*, Phys. Rev. B **54**, 14914 (1996).
11. T. Xiang, J.M. Wheatley, Phys. Rev. B **96**, R12653 (1996).
12. R. Eder *et al.*, Phys. Rev. B **55**, R3414 (1997).
13. F. Lema, A.A. Aligia, Phys. Rev. B **55**, 14092 (1997); F. Lema *et al.*, Phys. Rev. B **55**, 15295 (1997); P.W. Leung *et al.*, Phys. Rev. B **56**, 6320 (1997).
14. C. Kim *et al.*, Phys. Rev. Lett. **80**, 4245 (1998).
15. T. Tohyama *et al*, J. Phys. Soc. Jpn **69**, 9 (2000).
16. F. Ronning *et al.*, Science **282**, 2067 (1998).
17. F. Ronning *et al.*, to be published in Physica C (2000).
18. W. Hanke *et al.*, Phys. Rev. Lett. **85**, 824 (2000).
19. S.C. Zhang, Science **275**, 1089 (1997); S. Meixner *et al.*, Phys. Rev. Lett. **79**, 4902 (1997).
20. S. Pairault *et al.*, Phys. Rev. Lett. **80**, 5389 (1998); Eur. Phys. J. B **16**, 85 (2000).
21. W. Metzner, Phys. Rev. B **43**, 8549 (1991).
22. S.K. Sarker, J. Phys. C **21**, L667 (1988).
23. K. Becker, P. Fulde, J. Chem. Phys. **91**, 4223 (1989).
24. H.S. Wall, *Analytic theory of continued fractions*, p. 169, Chelsea Publishing Company (1948).
25. The complete result for G_J is available at www.Physik.Uni-Augsburg.DE/theo3/∼pbrune/confrac.
26. R. Preuss *et al.*, Phys. Rev. Lett. **75**, 1344 (1995); *ibid.* **79**, 1122 (1997).
27. D. Duffy *et al.*, Phys. Rev. B **56**, 5597 (1997).
28. S. LaRosa *et al.*, Phys. Rev. B **56**, R525 (1997).
29. C. Dürr *et al.*, preprint `cond-mat/0007283`.
30. M. Greven *et al.*, Phys. Rev. Lett. **72**, 1096 (1994).